

## APPLICATIONS OF TOUGH2 TO INFILTRATION OF LIQUIDS IN MEDIA WITH STRONG HETEROGENEITY

*Karsten Pruess and Emilio Antunez*

Earth Sciences Division, Lawrence Berkeley Laboratory  
University of California, Berkeley, California 94720

### Introduction

Much hydrogeological research during the last decade has focused on the heterogeneity of natural geologic media on different scales. Most of this work has dealt with flow and transport in single-phase, isothermal conditions. The present paper is concerned with multiphase and nonisothermal flows in strongly heterogeneous media. A primary driver of our studies is the hydrogeological system at Yucca Mountain, which is currently being evaluated by the Department of Energy for its suitability as the site of the first geologic repository for civilian high-level nuclear wastes in the U.S. Yucca Mountain is located in the arid Southwest, near the Nevada-California border. Going from large scale to small, formation heterogeneities at Yucca Mountain include (i) alternating tilting layers of welded and non-welded tuffs with different matrix permeability and variable degree of fracturing, (ii) major fault systems, (iii) well-connected and permeable fracture networks in low-permeability rocks, and (iv) individual fractures with highly variable apertures.

The potential repository horizon at Yucca Mountain is approximately 375 m beneath the land surface, in partially saturated, fractured rock; the water table is at a depth of approximately 600 m. Under present climatic conditions, rates of water infiltration at Yucca Mountain are small. There would be little concern about migration of water-soluble radionuclides if water flow proceeded in a uniform, volume-averaged manner. Concerns for site suitability and repository performance arise from potentially highly non-uniform water distribution and flow, which may be induced by the strong heterogeneities, especially fractures (Chesnut, 1994). Key issues involve the possible development of fast preferential flow paths, flow focusing, and localized water ponding. Numerical simulation experiments in computer-generated heterogeneous media are being used as a means to learn about water flow under partially saturated conditions with strong multi-scale heterogeneity.

Additional motivations for studying gravity-driven seepage of liquids in heterogeneous media arise in the context of water injection into depleted vapor-dominated geothermal reservoirs, and in environmental contamination problems involving non-aqueous phase liquids (NAPLs).

### Heterogeneous Media

Numerical simulation of a variety of fluid flow and heat transfer processes has been performed in media with different styles of heterogeneity (Figs. 1 - 3). Figure 1 shows a random distribution of low-permeability features in an otherwise homogeneous two-dimensional medium. This may represent a vertical section with silt bodies in a sandstone, or clay lenses in a soil. Figure 2 shows a layered medium, generated by means of the turning bands method (Tompson, 1989; Antunez and Pruess, 1994), with larger horizontal than vertical spatial correlation length. This style of heterogeneity is typical for sedimentary systems, such as clayey soils. For "small" fractures in hard rocks, essential features of aperture heterogeneity include (i) the presence of numerous asperity contacts between the fracture walls, (ii) a more or less gradual change from small apertures near the asperities to larger apertures away from the asperities, and (iii) significant local aperture variations due to wall roughness. A two-dimensional heterogeneous medium which may represent such fractures is shown in Fig. 3. It was also generated by means of the turning bands method, but specifying spatial correlation to be short-range. To obtain asperity contacts with zero apertures, the

log-normal aperture distribution used in the turning bands method was subjected to a linear shift,  $b \rightarrow b' = b - \Delta$ , and all  $b' < 0$  were reset to 0. The resulting distribution of asperities, idealized as regions of zero permeability, is shown in Fig. 4.

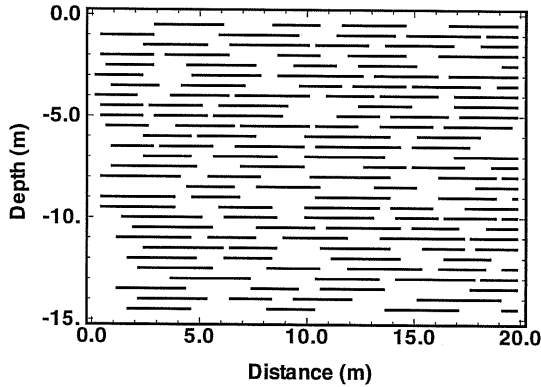


Figure 1. A heterogeneous medium, generated by random placement of horizontal impermeable obstacles, with lengths uniformly distributed in the range of 2 - 4 m.

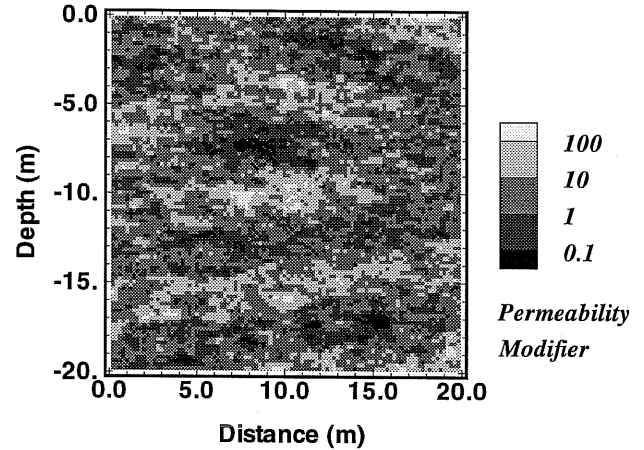


Figure 2. Log normally distributed permeability field, with spatial correlation lengths of  $\lambda_x = 0.8$  m,  $\lambda_z = 0.4$  m.

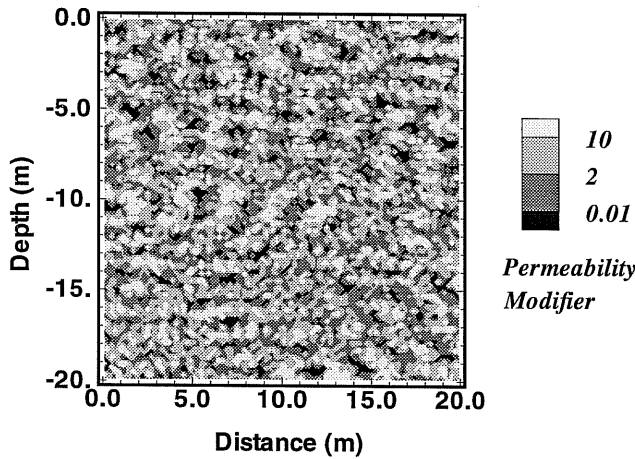


Figure 3. Stochastic permeability field, with correlation lengths of  $\lambda_x = 0.2$  m,  $\lambda_z = 0.1$  m.

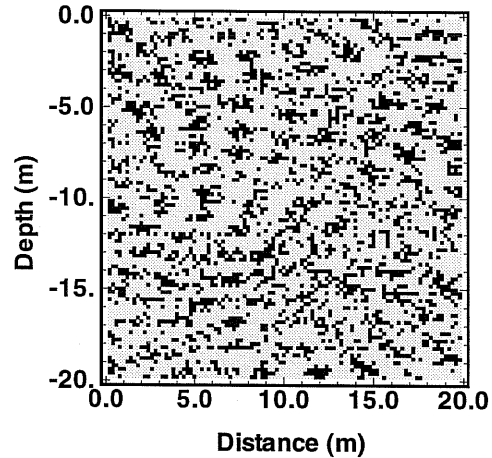


Figure 4. Distribution of asperity contacts in the permeability field of Fig. 3.

### Code Enhancements

Detailed resolution of small-scale heterogeneity requires thousands of grid blocks and leads to very demanding flow simulations. Using the recently developed preconditioned conjugate gradient module, TOUGH2 can handle systems with of the order of 10,000 grid blocks on workstations and PCs (Moridis and Pruess, 1995; Antunez et al., 1994). The code can model flow in heterogeneous media "as is;" all that is required is specification of an appropriate (large) number of domains with different properties in data block 'ROCKS'. However, specification of thousands

of different flow domains would be quite inconvenient as far as preparation of input data is concerned. Therefore, we have made some modifications in TOUGH2 to more conveniently deal with "strong" (grid-block-by-grid-block) heterogeneity. Additional revisions were made to address some new features in flow behavior that arise in strongly heterogeneous systems.

For flow systems with 10,000 or more grid blocks it is necessary to accommodate 5-digit element identification numbers. This requires changing the 1505 `FORMAT(20I4)` statements in subroutines `INPUT` and `RFILE`, file `t2f.f`, to `(16I5)`. To avoid having to specify large numbers of flow domains in problems with block-to-block permeability variation, we introduced an array of "permeability modifiers," `PM`. Externally generated `PM`-data, representing e.g. geostatistical realizations of spatially-correlated fields, can be conveniently fed into TOUGH2 as a floating point variable for each element through previously unused and available columns 41-50 in the 'ELEMEN' data block. We also coded provisions to optionally generate stochastic permeability modifiers internally. These modifiers are applied in subroutine `MULTI` as multiplicative factors to the permeabilities defined in block 'ROCKS'. This way, point-by-point permeability variation can be realized by specifying only one single set of domain data, which serves as a reference material. In addition to scaling absolute permeabilities according to  $k \rightarrow k' = k * PM$ , we simultaneously apply a consistent scaling of capillary pressures according to  $P_{cap} \rightarrow P_{cap}' = P_{cap}/SQRT(PM)$  (Leverett, 1941).

Flow simulations with strong (block-by-block) heterogeneity pose some difficulties that are not usually encountered when simulating the same fluid and heat flow processes in homogeneous media, or in media with only a few different domains. The variations in absolute permeability and strength of capillary pressure make intrinsic response times highly spatially variable. This complicates and lengthens the approach to steady states which are often desired as initial conditions for flow simulations. Potentially more serious problems may arise when in the course of a simulation certain grid blocks come very close to phase boundaries, and remain there for extended time periods. This can severely limit attainable time step sizes. Such occurrences are of course possible in much simpler, less heterogeneous systems. However, in systems with block-by-block variation of permeability fields these effects can be so frequent and persistent that some code revision may be necessary, to prevent time steps from being reduced to impractical levels. A more robust behavior can be achieved by broadening the phase change criterion from a "sharp" line to a finite-size window. For example, in the EOS4 fluid property module a transition from single-phase liquid to two-phase conditions is normally made when  $P < P_{gas}$  is encountered, where  $P_{gas}$  is the "bubbling" pressure. For some simulations of highly heterogeneous systems, we have revised this condition to  $P < P_{gas} * (1.-1.e-4)$ , i.e., we require pressure to drop below  $P_{gas}$  by a finite amount before allowing a gas phase to evolve.

## Numerical Experiments

Gravity-driven infiltration of water in the media shown in Figs. 1 - 3 was simulated with a new equation-of-state module, EOS9. This implements a Richards' equation-type approximation to saturated/unsaturated flow, which treats only single-component aqueous-phase flow, while the gas phase is treated as a passive bystander at constant pressure. Simulation parameters used are variations of a reference medium as given in Table 1; results are shown in Figs. 5 - 9.

### *Medium with Random Horizontal Obstacles*

Infiltration of an initially rectangular water plume in the medium of Fig. 1 shows a dendritic pattern of liquid migration when capillary pressures are neglected (Fig. 5). The impermeable obstacles divert flow sideways, causing the plume to broaden as it descends. A detailed analysis shows that plume broadening proceeds in analogy to Fickian diffusion, i.e., mean square plume size grows proportional to vertical distance traveled by the center-of-mass of the plume (Pruess, 1994). The heterogeneous medium behaves as an anisotropic dispersive medium; effective volume-averaged properties are found to be  $k_h = 7.5$  darcy,  $k_v = 1.2$  darcy, anisotropy ratio  $k_h/k_v = 6.3$ , and transverse dispersivity  $\alpha_T = 1.2$  m.

**Table 1. Parameters for test problems with detailed explicit heterogeneity.**

Reference permeability Porosity	$k = 10^{-11} \text{ m}^2$ (10 darcy) $\phi = 0.35$
Relative Permeability	
van Genuchten function for liquid (1980) $k_{rl} = \sqrt{S^*} \left\{ 1 - \left( 1 - [S^*]^{1/\lambda} \right)^\lambda \right\}^2$	$S^* = (S_l - S_{lr}) / (1 - S_{lr})$
Corey-curve for gas <sup>†</sup> $k_{rg} = (1 - \hat{S})^2 \left( 1 - [\hat{S}]^2 \right)$ irreducible water saturation irreducible gas saturation exponent	$\hat{S} = (S_l - S_{lr}) / (1 - S_{lr} - S_{gr})$ $S_{lr} = 0.15$ $S_{gr} = 0.05$ $\lambda = 0.457$
Capillary Pressure	
van Genuchten function (1980) $P_{cap} = -(\rho_w g/a) \left( [S^*]^{-1/\lambda} - 1 \right)^{1-\lambda}$ irreducible water saturation exponent strength coefficient	$S^* = (S_l - S_{lr}) / (1 - S_{lr})$ $S_{lr} = 0.0$ or $0.15$ $\lambda = 0.457$ $a = 5 \text{ m}^{-1}$

<sup>†</sup> used only when both liquid and gas phases are active

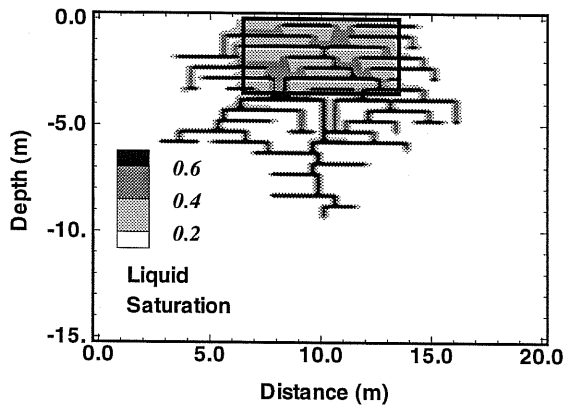


Figure 5. Water infiltration in the medium of Fig. 1, capillary pressures neglected. Initial water saturation is at irreducible level of  $S_l = 0.15$  throughout, except for the region outlined by the black rectangle where  $S_l = 0.99$ . Shading indicates water saturations after  $2 \times 10^5$  seconds.

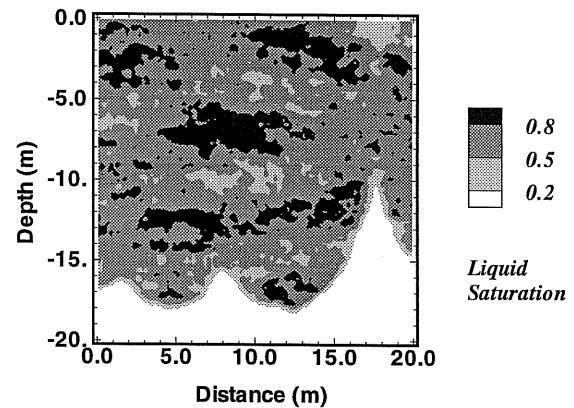


Figure 6. Water saturation in the medium of Fig. 2 after  $6 \times 10^5$  seconds of uniform infiltration applied at the top.

### Layered Medium

To study water infiltration in the layered medium of Fig. 2, we place a grid block with reference domain assignments (permeability modifier = 1) across the entire top of the domain. Water is injected into this block at a rate of 0.1 kg/s, which is approximately 6 % of the maximum unsaturated vertical water flow rate under unit head gradient. Water saturations after 6.9 days of infiltration, shown in Fig. 6, reflect the layering of the medium, with higher water saturations encountered in the less permeable layers where capillary effects are stronger. Capillary pressures at the injection boundary quickly reach a quasi-steady value of  $P_{cap} = -1830$  Pa. This capillary pressure is sufficiently negative to largely prevent water from entering the more highly permeable region that extends from 16.5 to 18.5 m distance at the top of the flow domain. The diminished infiltration over a portion of the boundary is seen to cast a “shadow” of diminished water saturations all the way down to the infiltration front.

### Small Fracture in Hard Rock

The heterogeneous medium shown in Fig. 3 serves as a model of a small fracture in hard rock, such as may be encountered in the tuff formations at Yucca Mountain. To study the behavior of liquid infiltration plumes, the entire flow domain is initialized with a uniform initial water saturation at the irreducible level of  $S_1 = 0.15$ , except for a square region at the top (extending from 6 to 14 m distance, and from 0 to -8 m depth) which is initialized as  $S_1 = 0.99$ . Fig. 7 shows the liquid saturation distribution after the initially square plume has evolved for a period of 4.6 days in response to gravity, capillary, and pressure forces. This simulation shows features that are reminiscent of field observations at Rainier Mesa, a possible analog to the Yucca Mountain site (Wang et al., 1993). In particular, we note the development of preferential, fingering flow, with significant ponding and bypassing. Fig. 8 shows an infiltration plume in the same fracture, which evolved from applying constant-rate injection at the top in the distance interval from 6 m to 14 m. The injection rate was specified in such a way that at the time of 4.6 days the fluid content of the plume in Fig. 8 is equal to that of Fig. 7. The infiltration patterns are quite different, indicating the sensitivity to boundary conditions in this highly gravitationally-unstable problem.

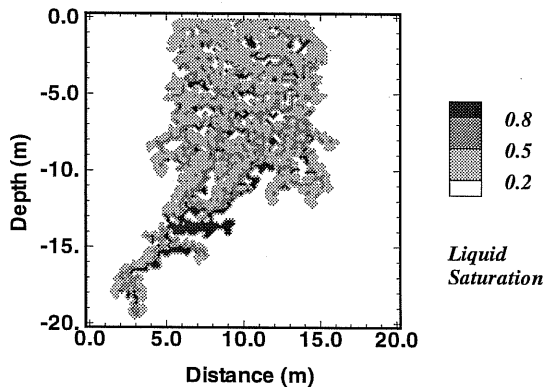


Figure 7. Water saturations in the medium of Fig. 3, shown 4.6 days after releasing a square plume of  $8 \times 8$  m<sup>2</sup> size from the top, center of the domain.

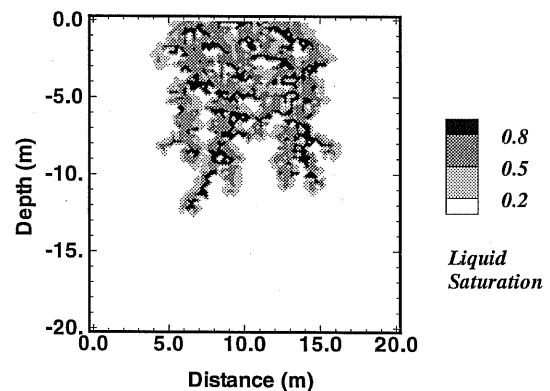


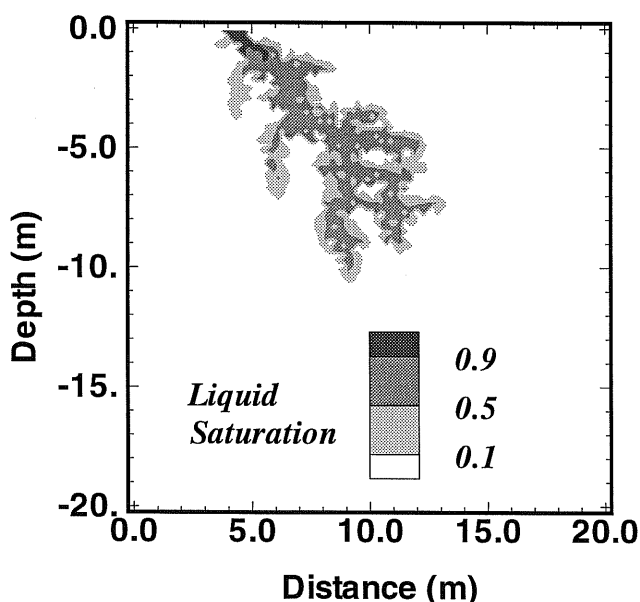
Figure 8. Same as Fig. 7, except here water was injected uniformly for 4.6 days at the top in the interval  $6 \text{ m} \leq x \leq 14 \text{ m}$ . Total water mass is equal to that in the plume in Fig. 7.

### Water Seepage through a Hot Fracture

The final study presented here was designed to explore thermo-hydrologic processes that would be encountered near the hot repository horizon at Yucca Mountain. A key issue is whether or not water seeping downward along sub-vertical fractures would fully vaporize as it traverses regions with temperatures above the nominal boiling point (96 °C at the repository elevation). The

basic flow system involves the heterogeneous vertical fracture shown in Fig. 3, with a reference permeability of  $10^{-10}$  m<sup>2</sup> over the assumed thickness of the 2-D section of 1 cm. The EOS4 fluid property module is used to represent vapor pressure lowering effects which can be very strong in processes involving (partial) dry-out. The fracture is initialized at a temperature of 110 °C, and is assumed to contain vapor (no air) in gravity equilibrium with an average pressure of 88.74 kPa. Even though vapor pressures are considerably below the saturated vapor pressure of 143.27 kPa at T = 110 °C, a small liquid saturation of approximately .013 % is present in the fracture due to strong vapor pressure lowering effects. The fracture walls are modeled as semi-infinite impermeable halfspaces, also initialized at a uniform above-boiling temperature of 110 °C. Water at a temperature of approximately 24 °C is then injected at the top of the fracture at a rate of 273.8 kg per day, and constant-pressure boundary conditions are maintained at the right edge of the fracture. The essential mechanism determining the fate of the injected water is heat exchange between the fracture and the wall rock, which is modeled here by means of the semi-analytical technique provided in TOUGH2.

The evolution of the liquid plume shows strong similarities to the behavior of water injection plumes in depleted zones of vapor-dominated geothermal reservoirs (Pruess, 1991; Pruess and Enezy, 1993; Pruess, 1995). Water descending in the fracture by gravitational force is partially vaporized from heat that is supplied conductively from the wall rock. Complex two-phase fluid flow and heat transfer processes develop, including vapor-liquid counterflows that provide a very efficient heat transfer mechanism akin to a heat pipe. Water boils throughout the hotter portions of the plume, while vapor condensation occurs in cooler regions. The general direction of vapor flow is towards the right constant-pressure boundary. The vapor pressure gradients associated with this flow cause the descending liquid plume to deviate from the predominant vertical direction and veer to the right (see Fig. 9).



Of the total liquid mass of 132.7 kg injected over an 11.63 hour period, an amount of 60.4 kg or 45.5 % has escaped vaporization, and has seeped over more than 10 m vertical distance through the hot fracture. Additional numerical experiments have shown that the fraction of water escaping vaporization increases with injection rate, as expected, reflecting limitations of conductive heat transfer from the wall rocks. Additional fully three-dimensional calculations have been initiated to include effects of water being imbibed by wall rocks of low but finite permeability.

Figure 9. Boiling infiltration plume after 11.63 hours of water injection into a highly heterogeneous, hot fracture (initial temperature 110 °C).

## Discussion and Conclusions

The recently developed package of preconditioned conjugate gradient solvers for TOUGH2 makes possible the simulation of complex multi-phase fluid and heat flow processes in highly heterogeneous media. For most of the flow problems presented here the Lanczos-type bi-conjugate gradient square solver (DSLUCS) provided a stable and efficient solution. However, the problem of water seepage through a hot fracture could only be solved with the bi-conjugate gradient method (DSLUBC), while DSLUCS as well as the generalized minimum residual method (DSLUGM) performed poorly.

Heterogeneity at different scales may be the key to understanding water flow, thermal loading effects, and radionuclide transport at Yucca Mountain. Using flow systems with of the order of 10,000 grid blocks we have been able to achieve a detailed resolution of spatially-correlated heterogeneities down to the decimeter scale. Numerical experiments of gravitationally unstable liquid infiltration in such media have revealed complex phenomenology, including fingering, ponding, and bypassing. Simulation capabilities have now reached a sophistication where detailed mechanistic models can be constructed to study issues that are critical to nuclear waste containment, such as fast preferential water flow in fractures.

## Acknowledgement

The authors appreciate helpful discussions with George Moridis. Thanks are due to Curt Oldenburg and Stefan Finsterle for a careful review of the manuscript. This work was carried out under U.S. Department of Energy Contract No. DE-AC03-76SF00098 for the Director, Office of Civilian Radioactive Waste Management, Yucca Mountain Site Characterization Project Office, and Office of External Relations, administered by the Nevada Operations Office, U.S. Department of Energy, in cooperation with the Swiss National Cooperative for the Disposal of Radioactive Waste (NAGRA).

## References

- Antunez, E. and K. Pruess. The Use of the Turning Bands Method (TBM) to Generate Stochastic Aperture Distributions in Heterogeneous Fractures. Lawrence Berkeley Laboratory Report LBL-35581, May 1994.
- Antunez, A., G. Moridis and K. Pruess. Large-Scale Geothermal Reservoir Simulation on PCs, Lawrence Berkeley Laboratory Report LBL-35192, presented at 19th Workshop on Geothermal Reservoir Engineering, Stanford University, Stanford, CA, January 1994.
- Chesnut, D.A. Dispersivity in Heterogeneous Permeable Media, Proceedings, Fifth Annual International High-Level Radioactive Waste Management Conference, Las Vegas, NV, Vol. 4, pp. 1822 - 1841, American Nuclear Society, La Grange Park, IL, May 1994.
- Leverett, M. C., Capillary Behavior in Porous Solids, *Trans. Soc. Pet. Eng. AIME*, 142, 152-169, 1941.
- Moridis, G. and K. Pruess. T2CG1: A Package of Preconditioned Conjugate Gradient Solvers for the TOUGH2 Family of Codes, Lawrence Berkeley Laboratory Report LBL-36235, Lawrence Berkeley Laboratory, Berkeley, CA, 1995.
- Pruess, K. Numerical Simulation of Water Injection into Vapor-Dominated Reservoirs. Paper accepted for presentation at World Geothermal Congress, Florence, Italy, May 1995.
- Pruess, K. On the Validity of a Fickian Diffusion Model for the Spreading of Liquid Infiltration Plumes in Partially Saturated Heterogeneous Media. Invited Paper, in: *Computational*

*Methods in Water Resources X*, Vol. 1, pp. 537 - 544, Kluwer Academic Publishers, Dordrecht, Boston, London, 1994.

Pruess, K. and S. Enezy. Numerical Modeling of Injection Experiments at The Geysers, Lawrence Berkeley Laboratory Report LBL-33423, presented at 18th Workshop on Geothermal Reservoir Engineering, Stanford University, Stanford, CA, January 26-28, 1993.

Pruess, K. Grid Orientation and Capillary Pressure Effects in the Simulation of Water Injection into Depleted Vapor Zones, *Geothermics*, 20 (5/6), 257-277, 1991.

Tompson, A.F.B. Implementation of the Three-Dimensional Turning Bands Random Field Generator, *Water Resources Res.*, Vol. 25, No. 10, pp. 2227 - 2243, 1989.

van Genuchten, M. Th. A Closed-Form Equation for Predicting the Hydraulic Conductivity of Unsaturated Soils, *Soil Sci. Soc. Am. J.*, Vol. 44, pp. 892-898, 1980.

Wang, J.S.Y., N.G.W. Cook, H.A. Wollenberg, C.L. Carnahan, I. Javandel, and C.F. Tsang. Geohydrologic Data and Models of Rainier Mesa and Their Implications to Yucca Mountain, Proceedings, Fourth Annual International High-Level Radioactive Waste Management Conference, Las Vegas, NV, Vol. 1, pp. 675 - 681, American Nuclear Society, La Grange Park, IL, April 1993.